Adaptive Space-Time-Spreading-Assisted Wideband CDMA Systems Communicating over Dispersive Nakagami-m Fading Channels

Lie-Liang Yang

School of Electronics and Computer Science, University of Southampton, Southampton SO17 1BJ, UK
Email: lly@ecs.soton.ac.uk

Lajos Hanzo

School of Electronics and Computer Science, University of Southampton, Southampton SO17 1BJ, UK
Email: lh@ecs.soton.ac.uk

In this contribution, the performance of wideband code-division multiple-access (W-CDMA) systems using space-time-spreading- (STS-) based transmit diversity is investigated, when frequency-selective Nakagami-m fading channels, multiuser interference, and background noise are considered. The analysis and numerical results suggest that the achievable diversity order is the product of the frequency-selective diversity order and the transmit diversity order. Furthermore, both the transmit diversity and the frequency-selective diversity have the same order of importance. Since W-CDMA signals are subjected to frequency-selective fading, the number of resolvable paths at the receiver may vary over a wide range depending on the transmission environment encountered. It can be shown that, for wireless channels where the frequency selectivity is sufficiently high, transmit diversity may be not necessitated. Under this case, multiple transmission antennas can be leveraged into an increased bitrate. Therefore, an adaptive STS-based transmission scheme is then proposed for improving the throughput of W-CDMA systems. Our numerical results demonstrate that this adaptive STS-based transmission scheme is capable of significantly improving the effective throughput of W-CDMA systems. Specifically, the studied W-CDMA system's bitrate can be increased by a factor of three at the modest cost of requiring an extra 0.4 dB or 1.2 dB transmitted power in the context of the investigated urban or suburban areas, respectively.

Keywords and phrases: CDMA, space-time spreading, Nakagami-m fading, transmit diversity.

1. BACKGROUND ON LINK ADAPTATION

It is widely recognised that the channel quality of wireless systems fluctuates over a wide range and hence it is irrealistic to expect that conventional nonadaptive systems might be able to provide a time-invariant grade of service. Hence in recent years various near-instantaneously adaptive-coding-and-modulation- (ACM-) assisted arrangements have been proposed [1, 2], which have found their way also into the high-speed downlink packet access (HSDPA) mode of the third-generation wireless systems [3] and in other adaptively reconfigurable multicarrier orthogonal frequency division multiplex (OFDM) systems [4] as well as into single-carrier and multi-carrier DS-CDMA schemes [5]. The family of multi-carrier systems is now widely considered to be the most potent candidate for the next-generation systems of wireless communications. The taxonomy of ACM schemes and a plethora of open research problems was detailed in [5, Chapter 1], hence here we refrain from detailing these issues. The philosophy of these ACM schemes is that instead of dropping a wireless call, they temporarily drop their throughput [3], when the instantaneous channel quality quantified in terms of the signal to interference-plus-noise ratio (SINR) [5] is too low and hence the resultant bit error ratio (BER) happens to be excessive. In this contribution, we will focus our attention on a less well-documented area of link adaptivity, namely, on the effects on multipath-induced dispersion-controlled adaptivity [5]. Achieving these ambitious objectives requires efficient

cross-layer design,[1] which supports the agile and prompt liaison of the OSI layers concerned, potentially requiring an interaction between the physical, network, and service layers, as it was exemplified in [3, 5]. More explicitly, in order to be able to pass on the benefits of the increased system throughput of these cross-layer optimised ACM-aided transceivers to the service layer in terms of improved video or speech quality, near-instantaneously adaptive speech codecs [6] and video codecs [7] are required. These speech and video codecs must have the ability to reconfigure themselves under the control of the near-instantaneous channel quality, such as the advanced multirate (AMR) speech codec or the H.26L multimedia source codec [8]. The interactions and performance benefits of cross-layer-optimised third-generation wireless systems employing adaptive beamforming were quantified in [3], while a host of further cross-layer optimisation issues were treated in [9, 10, 11, 12, 13, 14].

Against this background, in this contribution we focus our attention on a specific channel-quality controlled link adaptation algorithm, which allows the system to increase its effective throughput, as a function of the instantaneous channel quality with the aid of a novel combination of multiple-antenna-assisted transmitter and receiver diversity schemes. The capacity and the achievable data rate of wireless communication systems is limited by the time-varying characteristics of the channels. An efficient technique of combating the time-varying effects of wireless channels is employing diversity. In recent years, space-time coding has received much attention as an effective transmit diversity technique used for combating fading in wireless communications [15, 16, 17, 18]. Space-time-block-coding-assisted [16] transmit diversity has now been adapted as an optional diversity mode in the third-generation (3G) wireless systems known as IMT2000 using wideband code-division multiple-access (W-CDMA) [19, 20]. Inspired by space-time codes, in [21], an attractive transmit diversity scheme based on space-time spreading (STS) has been proposed by Hochwald et al. for employment in CDMA systems. The simple spreading philosophy of this scheme is portrayed in the schematic of Figure 1 and exemplified with the aid of the signal waveforms seen in Figure 2, both of which will be discussed in detail during our further discourse. An STS scheme designed for supporting two transmission antennas and one receiver antenna has also been included in the cdma2000 W-CDMA standard [20]. In [21], the performance of CDMA systems using STS has been investigated by Hochwald et al., when the channel is modelled either as a flat or as a frequency-selective Rayleigh fading channel in the absence of multiuser

interference. It was argued that the proposed STS scheme is capable of attaining the maximal achievable transmit diversity gain without using extra spreading codes and without an increased transmit power. Furthermore, the results recorded for transmission over frequency-selective Rayleigh fading channels by Hochwald et al. [21, Figure 4] show that when there is a sufficiently high number of resolvable paths, a CDMA system using a single transmit antenna and a conventional RAKE receiver is capable of achieving an adequate diversity gain.

Wideband CDMA channels are typically frequency-selective fading channels, having a number of resolvable paths. Therefore, in this contribution, first we investigate the performance of W-CDMA systems using STS-based transmit diversity, when encountering multipath Nakagami-m fading channels, multiuser interference, and background noise. A BER expression is derived, when Gaussian approximation [22, 23] of the multiuser interference and that of the multipath interference is invoked. This BER expression implies that the diversity order achieved is the product of the transmit diversity order and the frequency selective diversity order. Furthermore, the analysis and the numerical results show that both the STS and the frequency selectivity of the channel appear to have the same order of importance, especially when the power decay factor of the multipath intensity profile (MIP) [24] is low.

The frequency-selective frequency-domain transfer function of W-CDMA wireless channels may vary slowly, but often over a wide dynamic range when roaming in urban and suburban areas [25]. Therefore, the number of resolvable paths at the receiver can be modelled as a random variable distributed over a certain range, depending on the location of the receiver, where the number of resolvable paths varies slowly, as the receiver moves. Consequently, STS schemes designed on the basis of a low number of resolvable paths or based on the premise of encountering a constant number of resolvable paths may not achieve the maximum communication efficiency in terms of the effective throughput.

Motivated by the above arguments, in the second part of this contribution an adaptive STS-based transmission scheme is proposed and investigated, which adapts the mode of operation of its STS scheme and its corresponding data rate according to the near-instantaneous frequency selectivity information fed back from the receiver to the transmitter. Our numerical results show that this adaptive STS scheme is capable of efficiently exploiting the diversity potential provided by the channel's frequency selectivity, hence significantly improving the effective throughput of W-CDMA systems.

The remainder of this paper is organized as follows. In the next section, the W-CDMA system's model using STS and the channel model are described. Section 3 considers the detection of STS-based W-CDMA signals. In Section 4, we derive the corresponding BER expression and summarize our numerical results, while in Section 5 we describe the proposed adaptive STS scheme and investigate its BER performance. Finally, our conclusions are offered in Section 6.

---

[1]Cross-layer design constitutes a novel area of wireless system research, which is motivated by the fact that some elements of wireless systems, such as handovers and power control, do not fit into the classic seven-layer open system interconnection (OSI) architecture and hence an improved system performance may be achieved by jointly optimising several layers. In this contribution, the service layer, namely, the achievable data rate or video quality and voice quality, would be improved by the increased bitrate attained by the proposed system.
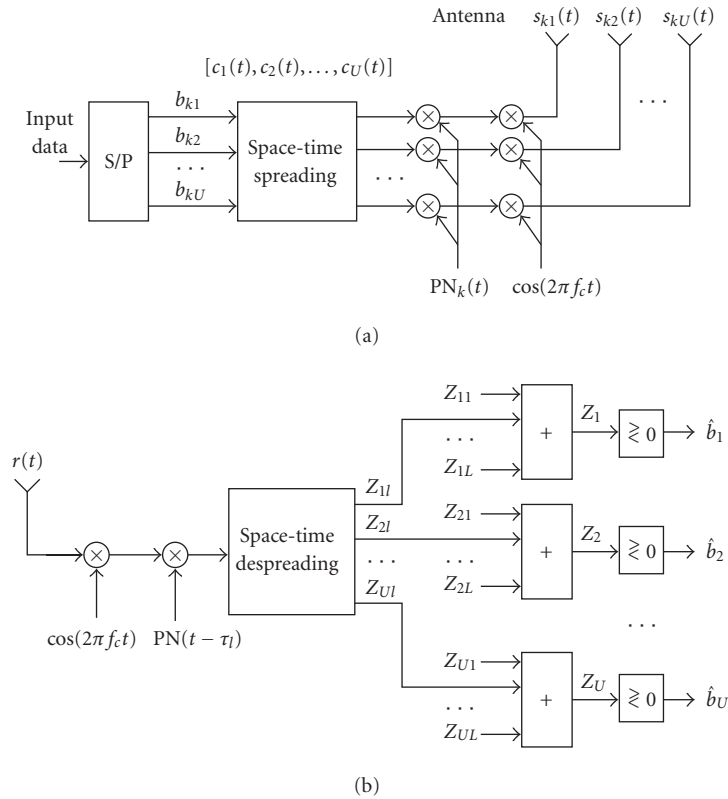
(a)

(b)

FIGURE 1: (a) Transmitter and (b) receiver block diagram of the W-CDMA system using space-time spreading.

2. SYSTEM MODEL

2.1. Transmitted signal

The W-CDMA system considered in this paper consists of U transmitter antennas and one receiver antenna. The transmitter schematic of the kth user and the receiver schematic of the reference user are shown in Figure 1, where real-valued data symbols using BPSK modulation and real-valued spreading [21] were assumed. Note that the analysis in this contribution can be extended to W-CDMA systems using U transmitter antennas and more than one receiver antenna, or to W-CDMA systems using complex-valued data symbols as well as complex-valued spreading. As shown in Figure 1a, at the transmitter side the binary input data stream having a bit duration of T_b is serial-to-parallel (S/P) converted to U parallel substreams. The new bit duration of each parallel substream, in other words the symbol duration, becomes $T_s = UT_b$. After S/P conversion, the U number of parallel bits are direct-sequence spread using the STS schemes proposed by Hochwald et al. [21] with the aid of U number of orthogonal spreading sequences—for example, Walsh codes—having a period of UG, where $G = T_b/T_c$ represents the number of chips per bit and T_c is the chip duration of the orthogonal spreading sequences. The STS scheme will be further discussed in detail during our forthcoming discourse in this section. As seen in Figure 1a, following STS, the U parallel signals to be mapped to the U transmission antennas are scrambled using the kth user's pseudonoise (PN)

sequence $PN_k(t)$, in order that the transmitted signals become randomised, and to ensure that the orthogonal spreading sequences employed within the STS block of Figure 1 can be reused by the other users. Finally, after the PN-sequence-based scrambling, the U number of parallel signals are carrier modulated and transmitted by the corresponding U number of antennas.

As described above, we have assumed that the number of parallel data substreams, the number of orthogonal spreading sequences used by the STS block of Figure 1, and the number of transmission antennas is the same, namely U. This specific STS scheme constitutes a specific subclass of the generic family of STS schemes, where the number of parallel data substreams, the number of orthogonal spreading sequences required by STS block, and the number of transmission antennas may take different values. The impressive study conducted by Hochwald et al. [21] has shown that the number of orthogonal spreading sequences required by STS is usually higher than the number of parallel substreams. The STS scheme having an equal number of parallel substreams, orthogonal STS-related spreading sequences, as well as transmission antennas constitutes an attractive scheme, since this STS scheme is capable of providing maximal transmit diversity without requiring extra STS spreading codes. Note that for the specific values of $U = 2, 4$ the above-mentioned attractive STS schemes have been specified by Hochwald et al. [21]. In this contribution, we only investigate these attractive STS schemes.
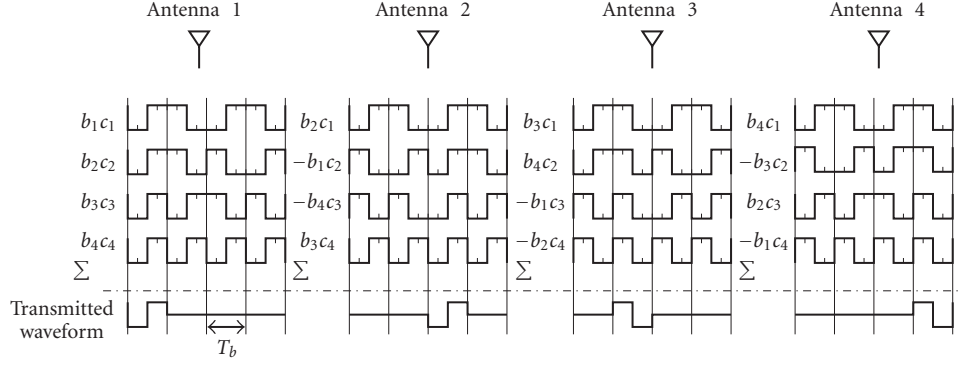
FIGURE 2: Illustration of STS using four transmission antennas transmitting 4 bits within $4T_b$ duration, where $b_1 = b_2 = b_3 = b_4 = +1$ were assumed. Furthermore, c_1, c_2, c_3, c_4 are four STS-related orthogonal codes having a period of $4T_b$. In this example, the STS-codes were chosen as follows: $c_1 = -1 -1 +1 +1\ +1 +1 -1 -1\ -1 -1 +1 +1\ +1 +1 -1 -1$, $c_2 = -1 -1 +1 +1\ +1 +1 -1 -1\ -1 +1 +1 -1 -1\ -1 -1 +1 +1 +1$, $c_3 = -1 -1 +1 +1\ -1 -1 +1 +1\ +1 +1 -1 -1 -1\ +1 +1 -1 -1$, $c_4 = -1 -1 +1 +1\ -1 -1 +1 +1\ -1 -1 +1 +1 +1\ -1 -1 +1 +1$. We note however that the codes used in Figure 3 could be also employed after repeating them four times without the loss of orthogonality.
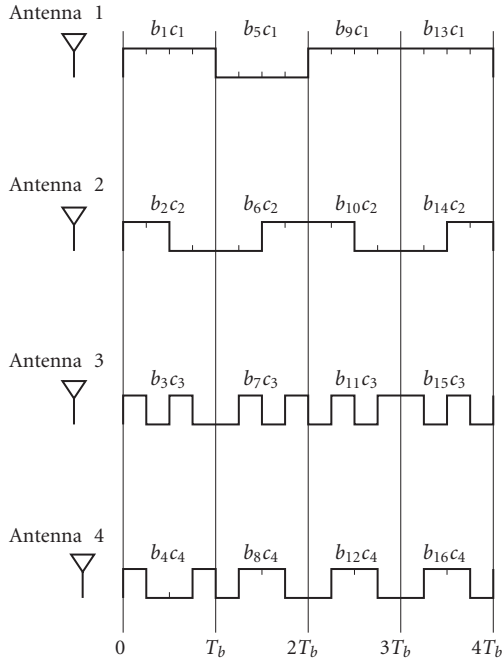

FIGURE 3: Illustration of the transmitted waveforms of the transmission scheme without using STS, that is, the four transmission antennas transmit their data independently. In this figure, we assumed that $b_1 = b_2 = b_3 = b_4 = +1$, $b_5 = b_6 = b_7 = b_8 = -1$, $b_9 = b_{10} = +1$, $b_{11} = b_{12} = -1$, $b_{13} = +1$, $b_{14} = +1$, $b_{15} = +1$, $b_{16} = -1$. Furthermore, c_1, c_2, c_3, c_4 are four STS-related orthogonal codes that have a reduced period of T_b, rather than $4T_b$ as it was in Figure 2 or $2T_b$ as in Figure 4. In this example, the STS-codes were chosen as follows: $c_1 = +1 +1 +1 +1$, $c_2 = +1 +1 -1 -1$, $c_3 = +1 -1 +1 -1$, $c_4 = +1 -1 -1 +1$.

Based on the philosophy of STS as discussed in [21] and referring to Figure 1a, the transmitted signal of the kth user can be expressed as

$$s_k(t) = \sqrt{\frac{2P}{U^2}} c(t) B_U(t) \times PN_k(t) \cos(2\pi f_c t), \qquad (1)$$

where P represents each user's transmitted power, which is constant for all users, $s_k(t) = \begin{bmatrix} s_{k1}(t) & s_{k2}(t) & \cdots & s_{kU}(t) \end{bmatrix}$ represents the transmitted signal vector of the U transmission antennas, while $PN_k(t)$ and f_c represent the DS-scrambling-based spreading waveform and the carrier frequency, respectively. The scrambling sequence waveform is given by $PN_k(t) = \sum_{j=-\infty}^{\infty} p_{kj} P_{T_c}(t - jT_c)$, where p_{kj} assumes values of $+1$ or -1 with equal probability, while $P_{T_c}(t)$ is the rectangular chip waveform, which is defined over the interval $[0, T_c)$. In (1), the vector $c(t) = \begin{bmatrix} c_1(t) & c_2(t) & \cdots & c_U(t) \end{bmatrix}$ is constituted by the U number of orthogonal signals assigned for the STS, $c_i(t) = \sum_{j=-\infty}^{\infty} c_{ij} P_{T_c}(t - jT_c)$, $i = 1, 2, \ldots, U$, denotes the individual components of the STS-based orthogonal spread signals, where $\{c_{ij}\}$ is an orthogonal sequence of period UG for each index i; $B_U(t)$ represents the $U \times U$-dimensional transmitted data matrix created by mapping U input data bits to the U parallel substreams according to the specific design rules outlined by Hochwald et al. [21], so that the maximum possible transmit diversity is achieved, while using relatively low-complexity signal detection algorithms. Specifically, $B_U(t)$ can be expressed as

$$B_U(t) = \begin{pmatrix} a_{11} b_{k,11} & a_{12} b_{k,12} & \cdots & a_{1U} b_{k,1U} \\ a_{21} b_{k,21} & a_{22} b_{k,22} & \cdots & a_{2U} b_{k,2U} \\ \vdots & \vdots & \ddots & \vdots \\ a_{U1} b_{k,U1} & a_{U2} b_{k,U2} & \cdots & a_{UU} b_{k,UU} \end{pmatrix}(t), \qquad (2)$$

where the time dependence of the (i, j)th element is indicated at the right-hand side of the matrix for simplicity. In (2), a_{ij} represents the sign of the element at the ith row and the jth column, which is determined by the STS design rule, while $b_{k,ij}$ is the data bit assigned to the (i, j)th element, which is one of the U input data bits $\{b_{k1}, b_{k2}, \ldots, b_{kU}\}$ of user k. Each input data bit of $\{b_{k1}, b_{k2}, \ldots, b_{kU}\}$ appears only once in any given row and in any given column. For $U = 2, 4$, $B_2(t)$, and
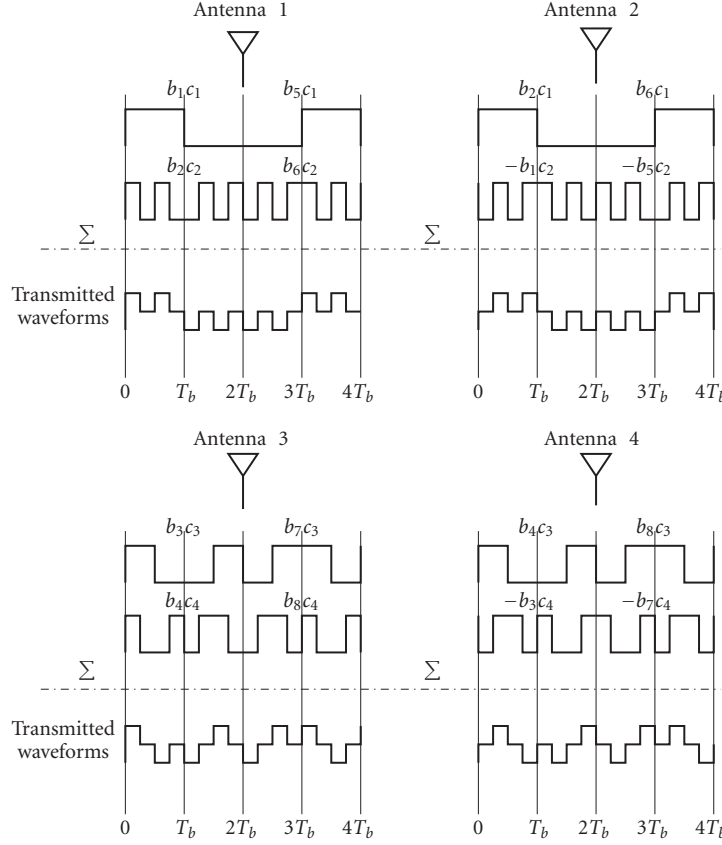
FIGURE 4: Illustration of STS using two transmission antennas transmitting 2 bits within $2T_b$ duration. Hence, four transmission antennas transmit 8 bits within $4T_b$ duration, where $b_1 = b_2 = b_3 = b_4 = +1$ and $b_5 = b_6 = b_7 = b_8 = -1$ were assumed. Furthermore, c_1, c_2, c_3, c_4 are four STS-related orthogonal codes that have a reduced period of $2T_b$, rather than $4T_b$ as it was in Figure 2. In this example, the STS codes were chosen as follows: $c_1 = +1 +1 +1 +1 \ -1 -1 -1 -1$, $c_2 = +1 -1 +1 -1 \ -1 +1 -1 +1$, $c_3 = +1 +1 -1 -1 \ -1 -1 +1 +1$, $c_4 = +1 -1 -1 +1 \ -1 +1 +1 -1$. We note however that the codes used in Figure 3 could be also employed after repeating them twice without the loss of orthogonality.

$\mathbf{B}_4(t)$ are given by [21]

$$\mathbf{B}_2(t) = \begin{pmatrix} b_{k1} & b_{k2} \\ b_{k2} & -b_{k1} \end{pmatrix}(t),$$

$$\mathbf{B}_4(t) = \begin{pmatrix} b_{k1} & b_{k2} & b_{k3} & b_{k4} \\ b_{k2} & -b_{k1} & b_{k4} & -b_{k3} \\ b_{k3} & -b_{k4} & -b_{k1} & b_{k2} \\ b_{k4} & b_{k3} & -b_{k2} & -b_{k1} \end{pmatrix}(t). \quad (3)$$

Based on (1) and (2) the signal transmitted by the uth antenna to the kth user can be explicitly expressed as

$$s_{ku}(t) = \sqrt{\frac{2P}{U^2}}[c_1(t)a_{1u}b_{k,1u}(t) + c_2(t)a_{2u}b_{k,2u}(t)$$
$$+ \cdots + c_U(t)a_{Uu}b_{k,Uu}(t)] \quad (4)$$
$$\times \mathrm{PN}_k(t)\cos(2\pi f_c t), \quad u = 1, 2, \ldots, U.$$

2.2. Channel model

The U number of parallel subsignals

$$\mathbf{s}_k(t) = [s_{k1}(t) \ \ s_{k2}(t) \ \ \cdots \ \ s_{kU}(t)] \quad (5)$$

is transmitted by the U number of antennas over frequency-selective fading channels, where each parallel subsignal experiences independent frequency-selective Nakagami-m fading. The complex lowpass equivalent representation of the impulse response experienced by the uth parallel subsignal of user k is given by [24]

$$h_k^u(t) = \sum_{l=1}^{L} h_{kl}^u \delta(t - \tau_{kl}) \exp(j\psi_{kl}^u), \quad (6)$$

where h_{kl}^u, τ_{kl}, and ψ_{kl}^u represent the attenuation factor, delay and phase shift of the lth multipath component of the channel, respectively, while L is the total number of resolvable multipath components and $\delta(t)$ is the Kronecker delta function. We assume that the phases $\{\psi_{kl}^u\}$ in (6) are independent identically distributed (i.i.d.) random variables uniformly distributed in the interval $[0, 2\pi)$, while the L

multipath attenuations $\{h_{kl}^u\}$ in (6) are independent Nakagami random variables with a probability density function (PDF) of [22, 23, 24, 25, 26, 27]

$$p(h_{kl}^u) = M(h_{kl}^u, m_{kl}^{(u)}, \Omega_{kl}^u),$$

$$M(R, m, \Omega) = \frac{2m^m R^{2m-1}}{\Gamma(m)\Omega^m} e^{(-m/\Omega)R^2}, \tag{7}$$

where $\Gamma(\cdot)$ is the gamma function [24], and $m_{kl}^{(u)}$ is the Nakagami-m fading parameter, which characterises the severity of the fading over the lth resolvable path [28] between the uth transmission antenna and user k. Furthermore, the parameter Ω_{kl}^u in (7) is defined as $\Omega_{kl}^u = E[(\alpha_{kl}^u)^2]$, which is assumed to be a negative exponentially decaying multipath intensity profile (MIP) given by $\Omega_{kl}^u = \Omega_{k1}^u e^{-\eta(l-1)}$, $\eta \geq 0$, where Ω_{k1}^u is the average signal strength corresponding to the first resolvable path and η is the rate of average power decay, while $(\alpha_{kl}^u)^2$ represents the individual coefficients of the MIP.

When supporting K asynchronous CDMA users and assuming perfect power control, the received complex lowpass equivalent signal can be expressed as

$$R(t) = \sum_{k=1}^{K} \sum_{l=1}^{L} \sqrt{\frac{2P}{U^2}} \mathbf{c}(t - \tau_{kl}) \mathbf{B}_U(t - \tau_{kl}) \mathbf{h}_{kl}$$
$$\times \mathrm{PN}_k(t - \tau_{kl}) + N(t), \tag{8}$$

where $N(t)$ is the complex-valued lowpass-equivalent additive white Gaussian noise (AWGN) having a double-sided spectral density of N_0, while

$$\mathbf{h}_{kl} = \begin{pmatrix} h_{kl}^1 \exp\left(j\psi_{kl}^1\right) \\ h_{kl}^2 \exp\left(j\psi_{kl}^2\right) \\ \vdots \\ h_{kl}^U \exp\left(j\psi_{kl}^U\right) \end{pmatrix}, \quad k = 1, 2, \ldots, K, \ l = 1, 2, \ldots, L, \tag{9}$$

represents the channel's complex impulse response in the context of the kth user and the lth resolvable path, where $\psi_{kl}^u = \phi_{kl}^u - 2\pi f_c \tau_{kl}$. Furthermore, in (8) we assumed that the signals transmitted by the U number of transmission antennas arrive at the receiver antenna after experiencing the same set of delays. This assumption is justified by the fact that in the frequency band of cellular system the propagation delay differences among the transmission antenna elements are on the order of nanoseconds, while the multipath delays are on the order of microseconds [21], provided that U is a relatively low number.

2.3. Receiver model

Let the first user be the user of interest and consider a receiver using space-time despreading as well as diversity combining, as shown in Figure 1b, where the subscript of the reference user's signal has been omitted for notational convenience. The receiver of Figure 1b carries out the inverse processing

of Figure 1a, in addition to multipath diversity combining. In Figure 1b, the received signal is first down-converted using the carrier frequency f_c, and then descrambled using the DS scrambling sequence of $\mathrm{PN}(t - \tau_l)$ in the context of the lth resolvable path, where we assumed that the receiver is capable of achieving near-perfect multipath-delay estimation for the reference user. The descrambled signal associated with the lth resolvable path is space-time despread using the approach of [21]—which will be further discussed in Section 3, in order to obtain U separate variables, $\{Z_{1l}, Z_{2l}, \ldots, Z_{Ul}\}$, corresponding to the U parallel data bits $\{b_1, b_2, \ldots, b_U\}$, respectively. Following space-time despreading, a decision variable is formed for each parallel transmitted data bit of $\{b_1, b_2, \ldots, b_U\}$ by combining the corresponding variables associated with the L number of resolvable paths, which can be expressed as

$$Z_u = \sum_{l=1}^{L} Z_{ul}, \quad u = 1, 2, \ldots, U. \tag{10}$$

Finally, the U number of transmitted data bits $\{b_1, b_2, \ldots, b_U\}$ can be decided based on the decision variables $\{Z_u\}_{u=1}^{U}$ using the conventional decision rule of a BPSK scheme.

Above we have described the transmitter model, the channel model, as well as the receiver model of W-CDMA using STS. We will now describe the detection procedure of the W-CDMA scheme using STS.

3. DETECTION OF SPACE-TIME SPREAD W-CDMA SIGNALS

Let $\mathbf{d}_l = \begin{bmatrix} d_{l1} & d_{l2} & \cdots & d_{lU} \end{bmatrix}^T$, $l = 1, 2, \ldots, L$, where T denotes vector transpose, represent the correlator's output variable vector in the context of the lth ($l = 1, 2, \ldots, L$) resolvable path, where

$$d_{ul} = \int_{\tau_l}^{UT_b + \tau_l} R(t) c_u(t - \tau_l) \mathrm{PN}(t - \tau_l) dt. \tag{11}$$

When substituting (8) into (11), it can be shown that

$$d_{ul} = \sqrt{2P} T_b \Big[a_{u1} b_{u1} h_l^1 \exp\left(j\psi_l^1\right) + a_{u2} b_{u2} h_l^2 \exp\left(j\psi_l^2\right) + \cdots + a_{uU} b_{uU} h_l^U \exp\left(j\psi_l^U\right) \Big]$$
$$+ J_u(l), \quad u = 1, 2, \ldots, U, \tag{12}$$

where

$$J_u(l) = J_{Su}(l) + J_{Mu}(l) + N_u(l), \quad u = 1, 2, \ldots, U, \tag{13}$$

and $J_{Su}(l)$ is due to the multipath-induced self-interference of the signal of interest inflicted upon the lth path signal, where $J_{Su}(l)$ can be expressed as

$$J_{Su}(l) = \sum_{j=1, j \neq l}^{L} \sqrt{\frac{2P}{U^2}} \int_{\tau_l}^{UT_b + \tau_l} \mathbf{c}(t - \tau_j) \mathbf{B}_U(t - \tau_j) \mathbf{h}_j \mathrm{PN}(t - \tau_j)$$
$$\times c_u(t - \tau_l) \mathrm{PN}(t - \tau_l) dt, \tag{14}$$

$J_{Mu}(l)$ represents the multiuser interference due to the signals transmitted simultaneously by the other users, which can be expressed as

$$J_{Mu}(l) = \sum_{k=2}^{K} \sum_{j=1}^{L} \sqrt{\frac{2P}{U^2}} \int_{\tau_l}^{UT_b+\tau_l} \mathbf{c}(t - \tau_{kj}) \mathbf{B}_U(t - \tau_{kj}) \tag{15}$$
$$\times \mathbf{h}_{kj} \, \text{PN}_k \, (t - \tau_{kj}) c_u(t - \tau_l) \, \text{PN}\,(t - \tau_l) dt,$$

and finally $N_u(l)$ is due to the AWGN, which can be written as

$$N_u(l) = \int_{\tau_l}^{UT_b+\tau_l} N(t) c_u(t - \tau_l) \, \text{PN}\,(t - \tau_l) dt, \tag{16}$$

which is a Gaussian distributed variable having zero mean and a variance of $2UN_0 T_b$.

Let $\mathbf{J}(l) = [J_1(l) \;\; J_2(l) \;\; \cdots \;\; J_U(l)]^T$. Then, the correlator's output variable vector $\mathbf{d}_l$ can be expressed as

$$\mathbf{d}_l = \sqrt{2P} T_b \mathbf{B}_U \mathbf{h}_l + \mathbf{J}(l), \quad l = 1, 2, \ldots, L, \tag{17}$$

where $\mathbf{B}_U$ is the reference user's $U \times U$-dimensional transmitted data matrix, which is given by (2), but ignoring the time dependence, while $\mathbf{h}_l$ is the channel's complex impulse

response between the base station and the reference user, as shown in (9) in the context of the reference user.

The attractive STS schemes of Hochwald et al. have the property [21] of $\mathbf{B}_U \mathbf{h}_l = \mathbf{H}_U \mathbf{b}$, that is, (17) can be written as

$$\mathbf{d}_l = \sqrt{2P} T_b \mathbf{H}_U \mathbf{b} + \mathbf{J}(l), \tag{18}$$

where $\mathbf{b} = [b_1 \;\; b_2 \;\; \cdots \;\; b_U]^T$ represents the U number of transmitted data bits, while $\mathbf{H}_U$ is a $U \times U$-dimensional matrix with elements from $\mathbf{h}_l$. Each element of $\mathbf{h}_l$ appears once and only once in a given row and also in a given column of the matrix $\mathbf{H}_U$ [21]. The matrix $\mathbf{H}_U$ can be expressed as

$$\mathbf{H}_U(l) = \begin{pmatrix} \alpha_{11}(l) & \alpha_{12}(l) & \cdots & \alpha_{1U}(l) \\ \alpha_{21}(l) & \alpha_{22}(l) & \cdots & \alpha_{2U}(l) \\ \vdots & \vdots & \ddots & \vdots \\ \alpha_{U1}(l) & \alpha_{U2}(l) & \cdots & \alpha_{UU}(l) \end{pmatrix}, \tag{19}$$

where $\alpha_{ij}(l)$ takes the form of $d_{ij} h_l^m \exp(j\psi_l^m)$, and $d_{ij} \in \{+1, -1\}$ represents the sign of the (i, j)th element of $\mathbf{H}_U$, while $h_l^m \exp(j\psi_l^m)$ belongs to the mth element of $\mathbf{h}_l$. For $U = 2, 4$, with the aid of [21], it can be shown that

$$\mathbf{H}_2(l) = \begin{pmatrix} h_l^1 \exp(j\psi_l^1) & h_l^2 \exp(j\psi_l^2) \\ -h_l^2 \exp(j\psi_l^2) & h_l^1 \exp(j\psi_l^1) \end{pmatrix},$$

$$\mathbf{H}_4(l) = \begin{pmatrix} h_l^1 \exp(j\psi_l^1) & h_l^2 \exp(j\psi_l^2) & h_l^3 \exp(j\psi_l^3) & h_l^4 \exp(j\psi_l^4) \\ -h_l^2 \exp(j\psi_l^2) & h_l^1 \exp(j\psi_l^1) & -h_l^4 \exp(j\psi_l^4) & h_l^3 \exp(j\psi_l^3) \\ -h_l^3 \exp(j\psi_l^3) & h_l^4 \exp(j\psi_l^4) & h_l^1 \exp(j\psi_l^1) & -h_l^2 \exp(j\psi_l^2) \\ -h_l^4 \exp(j\psi_l^4) & -h_l^3 \exp(j\psi_l^3) & h_l^2 \exp(j\psi_l^2) & h_l^1 \exp(j\psi_l^1) \end{pmatrix}. \tag{20}$$

With the aid of the analysis in [21], it can be shown that the matrix $\mathbf{H}_U(l)$ has the property of $\text{Re}\{\mathbf{H}_U^\dagger(l)\mathbf{H}_U(l)\} = \mathbf{h}_l^\dagger \mathbf{h}_l \cdot \mathbf{I}$, where $\dagger$ denotes complex conjugate transpose and $\mathbf{I}$ represents a $U \times U$-dimensional unity matrix. Letting $\mathbf{h}_u(l)$ denote the uth column of $\mathbf{H}_U(l)$, the variable Z_{ul} in (10) can be expressed as [21]

$$Z_{ul} = \text{Re}\{\mathbf{h}_u^\dagger(l)\mathbf{d}_l\} = \sqrt{2P} T_b b_u \sum_{u=1}^{U} |h_l^u|^2 + \text{Re}\{\mathbf{h}_u^\dagger(l)\mathbf{J}(l)\},$$
$$u = 1, 2, \ldots, U. \tag{21}$$

Finally, according to (10) the decision variables associated

with the U parallel transmitted data bits $\{b_1, b_2, \ldots, b_U\}$ of the reference user can be expressed as

$$Z_u = \sqrt{2P} T_b b_u \sum_{l=1}^{L} \sum_{u=1}^{U} |h_l^u|^2 + \sum_{l=1}^{L} \text{Re}\{\mathbf{h}_u^\dagger(l)\mathbf{J}(l)\}, \tag{22}$$
$$u = 1, 2, \ldots, U,$$

which shows that the receiver is capable of achieving a diversity order of UL, as indicated by the related sums of the first term.

Above we have analysed the detection procedure applicable to W-CDMA signals generated using STS. We will now derive the corresponding BER expression.

4. BER PERFORMANCE

4.1. BER analysis

In this section, we derive the BER expression of the STS-assisted W-CDMA system by first analysing the statistics of the variable Z_u, $u = 1, 2, \ldots, U$, with the aid of the Gaussian approximation [23]. According to (22), for a given set of complex channel transfer factor estimates $\{h_l^u\}$, Z_u can be approximated as a Gaussian variable having a mean given by

$$\mathrm{E}[Z_u] = \sqrt{2P} T_b b_u \sum_{l=1}^{L} \sum_{u=1}^{U} |h_l^u|^2. \tag{23}$$

Based on the assumption that the interferences imposed by the different users, by the different paths, as well as by the AWGN constitute independent random variables, the variance of Z_u can be expressed as

$$\mathrm{Var}[Z_u] = \mathrm{E}\left[\left(\sum_{l=1}^{L} \mathrm{Re}\left\{\mathbf{h}_u^\dagger(l)\mathbf{J}(l)\right\}\right)^2\right]$$
$$= \sum_{l=1}^{L} \mathrm{E}\left[\left(\mathrm{Re}\left\{\mathbf{h}_u^\dagger(l)\mathbf{J}(l)\right\}\right)^2\right] \tag{24}$$
$$= \frac{1}{2} \sum_{l=1}^{L} \mathrm{E}\left[\left(\mathbf{h}_u^\dagger(l)\mathbf{J}(l)\right)^2\right].$$

Substituting $\mathbf{h}_u(l)$, which is the uth column of $\mathbf{H}_u(l)$ in (19), and $\mathbf{J}(l)$ having elements given by (13) into the above equation, it can be shown that for a given set of channel estimates $\{h_l^u\}$, (24) can be simplified as

$$\mathrm{Var}[Z_u] = \frac{1}{2} \sum_{l=1}^{L} \sum_{u=1}^{U} |h_l^u|^2 \mathrm{E}\left[\left(J_u(l)\right)^2\right]$$
$$= \frac{1}{2} \sum_{l=1}^{L} \sum_{u=1}^{U} |h_l^u|^2 \mathrm{Var}[J_u(l)], \tag{25}$$

where $J_u(l)$ is given by (13). In deriving (25) we exploited the assumption of $\mathrm{Var}[J_1(l)] = \mathrm{Var}[J_2(l)] = \cdots = \mathrm{Var}[J_U(l)]$.

As shown by Hochwald et al. in (13), $J_u(l)$ consists of three terms, namely the AWGN $N_u(l)$ having a variance of $2UN_0T_b$, $J_{Su}(l)$, which is the multipath-induced self-interference inflicted upon the lth path of the user of interest, and $J_{Mu}(l)$ imposed by the $(K-1)$ interfering users. By careful observation of (14), it can be shown that $J_{Su}(l)$ consists of U^2 terms and each term takes the form of $\sum_{j=1, j \neq l}^{L} \sqrt{2P/U^2} \int_{\tau_l}^{UT_b+\tau_l} c_m(t - \tau_j)a_{mn}b_{mn}(t - \tau_j)h_j^n \exp(j\psi_j^n) \mathrm{PN}(t - \tau_j) \times c_u(t - \tau_l) \mathrm{PN}(t - \tau_l)dt$. Assuming that $\mathrm{E}[(h_j^n)^2] = \Omega_1 e^{-\eta(j-1)}$, that is, that $\mathrm{E}[(h_j^n)^2]$ is independent of the index of the transmission antenna, and following the analysis in [22], it can be shown that the above term has a variance of $2\Omega_1 E_b T_b[q(L,\eta)-1]/(GU)$, where $q(L,\eta) = (1 - e^{-L\eta})/(1 - e^{-\eta})$, if $\eta \neq 0$ and $q(L,\eta) = L$, if $\eta = 0$. Consequently, we have $\mathrm{Var}[J_{Su}(l)] =$

$U^2 \times 2\Omega_1 E_b T_b[q(L,\eta)-1]/(GU) = 2U\Omega_1 E_b T_b[q(L,\eta)-1]/G$. Similarly, the multiuser interference term $J_{Mu}(l)$ of (15) also consists of U^2 terms, and each term has the form of $\sum_{k=2}^{K} \sum_{j=1}^{L} \sqrt{2P/U^2} \int_{\tau_l}^{UT_b+\tau_l} c_m(t - \tau_{kj})a_{mn}b_{mn}(t - \tau_{kj})h_{kj}^n \exp(j\psi_{kj}^n) \mathrm{PN}_k(t - \tau_{kj})c_u(t - \tau_l) \mathrm{PN}(t - \tau_l)dt$. Again, with the aid of the analysis in [22], it can be shown that this term has the variance of $(K - 1)4\Omega_1 E_b T_b q(L,\eta)/(3GU)$, and consequently the variance of $J_{Mu}(l)$ is given by $\mathrm{Var}[J_{Mu}(l)] = (K - 1)4U\Omega_1 E_b T_b q(L,\eta)/(3G)$. Therefore, the variance of $J_u(l)$ can be expressed as

$$\mathrm{Var}[J_u(l)] = 2N_0UT_b + \frac{2U\Omega_1 E_b T_b[q(L,\eta)-1]}{G}$$
$$+ \frac{(K-1)4U\Omega_1 E_b T_b q(L,\eta)}{3G}, \tag{26}$$

and the variance of Z_u for a given set of channel estimates $\{h_l^u\}$ can be expressed as

$$\mathrm{Var}[Z_u] = \sum_{l=1}^{L} \sum_{u=1}^{U} |h_l^u|^2 \Bigg[N_0UT_b + \frac{U\Omega_1 E_b T_b[q(L,\eta)-1]}{G}$$
$$+ \frac{(K-1)2U\Omega_1 E_b T_b q(L,\eta)}{3G} \Bigg]. \tag{27}$$

Based on (23) and (27), the BER conditioned on h_l^u for $u = 1, 2, \ldots, U$ and $l = 1, 2, \ldots, L$ can be written as

$$P_b(E|\{h_l^u\}) = Q\left(\sqrt{\frac{\mathrm{E}^2[Z_u]}{\mathrm{Var}[Z_u]}}\right) = Q\left(\sqrt{2 \cdot \sum_{l=1}^{L} \sum_{u=1}^{U} \gamma_{lu}}\right), \tag{28}$$

where $Q(x)$ represents the Gaussian Q-function, which can also be represented in its less conventional form as $Q(x) = (1/\pi) \int_0^{\pi/2} \exp(-x^2/2\sin^2\theta)d\theta$, where $x \geq 0$ [28, 29]. Furthermore, γ_{lu} in (28) is given by

$$\gamma_{lu} = \bar{\gamma}_c \cdot \frac{(h_l^u)^2}{\Omega_1},$$
$$\bar{\gamma}_c = \frac{1}{U}\left[\frac{(2K+1)q(L,\eta)-3}{3G} + \left(\frac{\Omega_1 E_b}{N_0}\right)^{-1}\right]^{-1}. \tag{29}$$

The average BER, $P_b(E)$, can be obtained by averaging the conditional BER of (28) over the joint PDF of the instantaneous SNR values corresponding to the L multipath components and to the U transmit antennas $\{\gamma_{lu} : l = 1, 2, \ldots, L; u = 1, 2, \ldots, U\}$. Since the random variables $\{\gamma_{lu} : l = 1, 2, \ldots, L; u = 1, 2, \ldots, U\}$ are assumed to be statistically independent, the average BER can be expressed as [30, (23)]

$$P_b(E) = \frac{1}{\pi} \int_0^{\pi/2} \prod_{l=1}^{L} \prod_{u=1}^{U} I_{lu}(\bar{\gamma}_{lu}, \theta)d\theta, \tag{30}$$
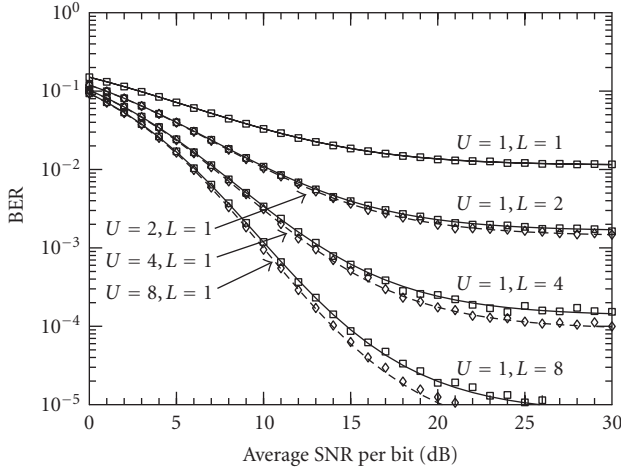
FIGURE 5: BER versus the SNR per bit, E_b/N_0, performance comparison between the space-time-spreading-based transmit diversity scheme and the conventional RAKE receiver arrangement using only one transmission antenna when communicating over flat-fading (for space-time spreading) and multipath (for RAKE) Rayleigh fading ($m_l = m_c = 1$) channels evaluated from (35) by assuming that the average power decay rate was $\eta = 0$. The solid line indicates the BER of the receiver-diversity-aided schemes, while the dashed line that of the transmit-diversity-assisted schemes ($G = 128, K = 10$).
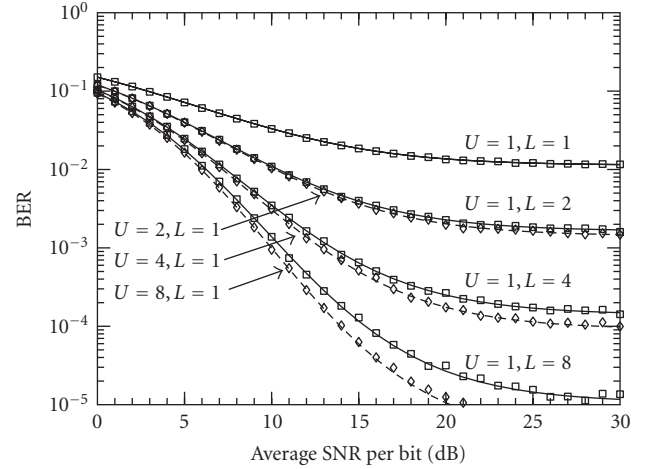

FIGURE 6: BER versus the SNR per bit, E_b/N_0, performance comparison between the space-time-spreading-based transmit diversity scheme and the conventional RAKE receiver arrangement using only one transmission antenna when communicating over flat-fading (for space-time spreading) and multipath (for RAKE) Rayleigh fading ($m_l = m_c = 1$) channels evaluated from (35) by assuming that the average power decay rate was $\eta = 0.2$. The solid line indicates the BER of the receiver-diversity-aided schemes, while the dashed line that of the transmit-diversity-assisted schemes ($G = 128, K = 10$).

where

$$I_{lu}(\overline{\gamma}_{lu}, \theta) = \int_0^\infty \exp\left(-\frac{\gamma_{lu}}{\sin^2 \theta}\right) p_{\gamma_{lu}}(\gamma_{lu}) d\gamma_{lu}. \tag{31}$$

Since $\gamma_{lu} = \overline{\gamma}_c \cdot ((h_l^u)^2/\Omega_1)$ and h_l^u obeys the Nakagami-m distribution characterised by (7), it can be shown that the PDF of γ_{lu} can be expressed as

$$p_{\gamma_{lu}}(\gamma_{lu}) = \left(\frac{m_l^{(u)}}{\overline{\gamma}_{lu}}\right)^{m_l^{(u)}} \frac{\gamma^{m_l^{(u)}-1}}{\Gamma(m_l^{(u)})} \exp\left(-\frac{m_l^{(u)}\gamma_{lu}}{\overline{\gamma}_{lu}}\right), \quad \gamma_{lu} \geq 0, \tag{32}$$

where $\overline{\gamma}_{lu} = \overline{\gamma}_c e^{-\eta(l-1)}$ for $l = 1, 2, \ldots, L$.

Upon substituting (32) into (31) it can be shown that [28]

$$I_{lu}(\overline{\gamma}_{lu}, \theta) = \left(\frac{m_l^{(u)} \sin^2 \theta}{\overline{\gamma}_{lu} + m_l^{(u)} \sin^2 \theta}\right)^{m_l^{(u)}}. \tag{33}$$

Finally, upon substituting (33) into (30), the average BER of the STS-assisted W-CDMA system using U transmission antennas can be expressed as

$$P_b(E) = \frac{1}{\pi} \int_0^{\pi/2} \prod_{l=1}^{L} \prod_{u=1}^{U} \left(\frac{m_l^{(u)} \sin^2 \theta}{\overline{\gamma}_{lu} + m_l^{(u)} \sin^2 \theta}\right)^{m_l^{(u)}} d\theta, \tag{34}$$

which shows that the diversity order achieved is LU—the product of the transmit diversity order and the frequency-selective diversity order. Furthermore, if we assume that $m_l^{(u)}$ is independent of u, that is, that all of the parallel transmitted subsignals experience an identical Nakagami fading, then (34) can be expressed as

$$P_b(E) = \frac{1}{\pi} \int_0^{\pi/2} \prod_{l=1}^{L} \left(\frac{m_l \sin^2 \theta}{\overline{\gamma}_{lu} + m_l \sin^2 \theta}\right)^{U m_l} d\theta. \tag{35}$$

4.2. Numerical results and discussions

In Figures 5, 6, 7, 8, and 9 we compare the BER performance of the STS-assisted W-CDMA system transmitting over flat-fading channels and that of the conventional RAKE receiver using only one transmission antenna, but communicating over frequency-selective fading channels. The results in these figures were all evaluated from (35) by assuming appropriate parameters, which are explicitly shown in the corresponding figures. In Figures 5, 6, and 7 the BER was drawn against the SNR/bit, namely E_b/N_0, while in Figures 8 and 9 the BER was drawn against the number of users, K, supported by the system. From the results we observe that for transmission over Rayleigh fading channels ($m_l = 1$), as characterised by Figures 5, 6, and 8, both the STS-based transmit diversity scheme transmitting over the frequency-nonselective Rayleigh fading channel and the conventional RAKE receiver scheme communicating over frequency-selective Rayleigh fading channels
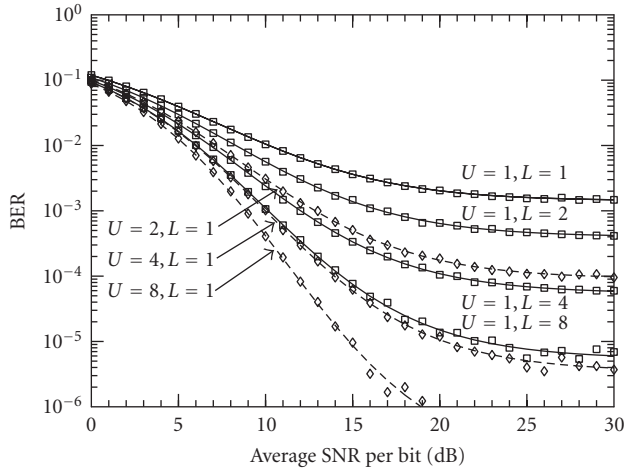
Figure 7: BER versus the SNR per bit, E_b/N_0, performance comparison between the space-time-spreading-based transmit diversity scheme and the conventional RAKE receiver arrangement using only one transmission antenna when communicating over flat-fading (for space-time spreading) and multipath (for RAKE) Nakagami-m fading channels evaluated from (35) by assuming that the average power decay rate was $\eta = 0.2$, where $m_1 = 2$ indicates that the first resolvable path constitutes a moderately fading path, while the other resolvable paths experience more severe Rayleigh fading ($m_c = 1$). The solid line indicates the BER of the receiver-diversity-aided schemes, while the dashed line that of the transmit-diversity-assisted schemes ($G = 128, K = 10$).

—— Frequency-selective diversity
--- Transmit diversity

Figure 8: BER versus the number of users, K, performance comparison between the space-time-spreading-based transmit diversity scheme and the conventional RAKE receiver arrangement using only one transmission antenna when communicating over flat-fading (for space-time spreading) and multipath (for RAKE) Rayleigh fading channels evaluated from (35) by assuming that the average power decay rate was $\eta = 0$ ($G = 128, E_b/N_0 = 20$ dB, $m_1 = m_c = 1$).

having the same number of resolvable paths as the number of transmission antennas in the STS-assisted scheme achieved a similar BER performance, with the STS scheme slightly outperforming the conventional RAKE scheme. For transmission over general Nakagami-m fading channels, if the first resolvable path is less severely faded, than the other resolvable paths, such as in Figures 7 and 9 where $m_1 = 2$ and $m_2 = m_3 = \cdots = m_c = 1$, the STS-based transmit diversity scheme communicating over the frequency-nonselective Rayleigh fading channel may significantly outperform the corresponding conventional RAKE-receiver-assisted scheme communicating over frequency-selective Rayleigh fading channels. This is because the STS-based transmit diversity scheme communicated over a single nondispersive path, which benefited from having a path experiencing moderate fading. However, if the number of resolvable paths is sufficiently high, the conventional RAKE receiver scheme is also capable of achieving a satisfactory BER performance.

Above we assumed that the number of resolvable paths was one, if the STS using more than one antenna was considered. By contrast, the number of resolvable paths was equal to the number of transmit antennas of the corresponding STS-based system, when the conventional RAKE receiver was considered. However, in practical W-CDMA systems the number of resolvable paths of each antenna's transmitted signal depends on its transmission environment. The number of resolvable paths dynamically changes, as the mobile
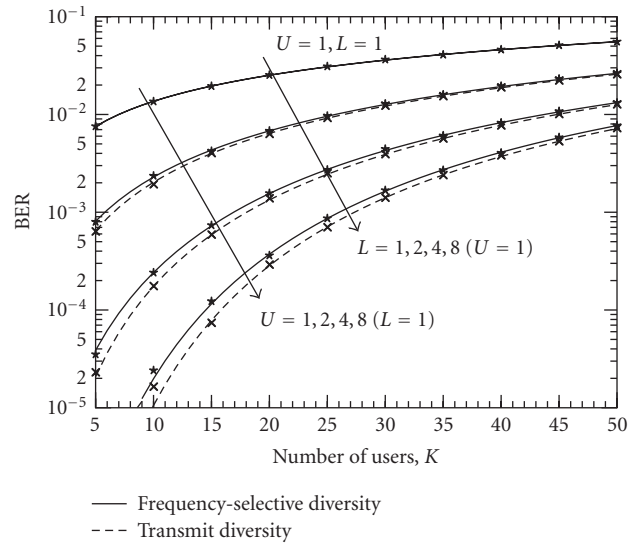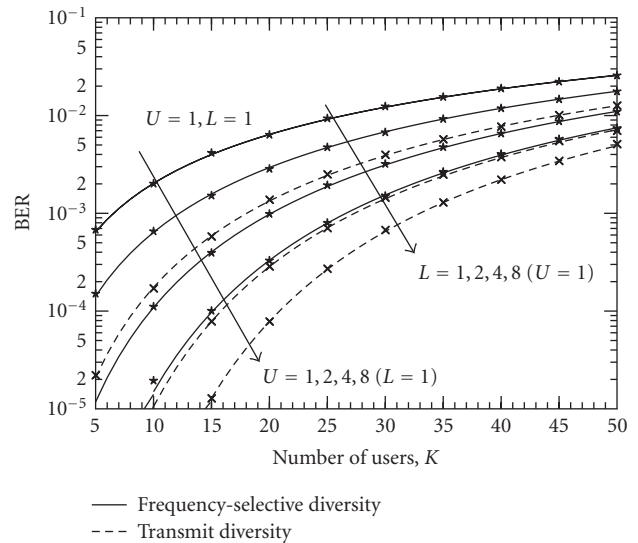

—— Frequency-selective diversity
--- Transmit diversity

Figure 9: BER versus the number of users, K, performance comparison between the space-time-spreading-based transmit diversity scheme and the conventional RAKE receiver arrangement using only one transmission antenna when communicating over the flat-fading (for space-time spreading) and multipath (for RAKE) Nakagami-m fading channels evaluated from (35) by assuming that the average power decay rate was $\eta = 0.2$, where $m_1 = 2$ indicates that the first resolvable path constitutes a moderately fading path, while the other resolvable paths experience more severe Rayleigh fading ($m_c = 1$); $G = 128, E_b/N_0 = 20$ dB.

traverses through different transmission environments. Specifically, in some scenarios the number of paths may be as low as $L = 1$, and in other scenarios it may be as high as $L > 10$. When the number of resolvable paths is as low as $L = 1$ or 2, employing STS-based transmit diversity is particularly valuable. However, when the number of resolvable paths is reasonably high, for example, $L > 4$, the employment of STS-based transmit diversity may not be necessary. An attractive approach is to adapt the mode of operation of the STS scheme, which is discussed in the following section.

5. DISPERSION-CONTROLLED ADAPTIVE SPACE-TIME SPREADING

The main philosophy behind the proposed channel-induced dispersion-controlled adaptive STS scheme is the real-time balancing of the link budget through the adaptive control of the STS-based transmission scheme, in order that the system achieves its maximum throughput, while maintaining the required target BER performance. More specifically, in this treatise we will aim for maintaining a target BER of 10^{-4}, regardless of the instantaneous channel quality experienced and exploit the improved channel quality provided by a higher number of resolvable multipath components experienced in scattering rich outdoor channels for increasing the system's effective throughput, ultimately leading to a potentially better speech [6] or video [7] quality for the users of the system.

In the context of the STS-assisted W-CDMA system, the delay spread of the wireless channels, and hence the number of resolvable paths, varies slowly over a range spanning from one to dozens of paths. The STS scheme designed based on a low number of resolvable paths, or even based on a relatively high but constant number of resolvable paths, cannot maximise the achievable throughput. For example, if the STS scheme is designed based on a low number of resolvable paths, in order to guarantee a required quality of service (QoS), the practically achieved QoS may be excessive, when the number of resolvable paths is high, provided that these resolvable paths are efficiently combined. However, if only a low but constant number of resolvable paths is combined, the diversity potential provided by the high number of resolvable paths is inevitably wasted. A high-efficiency STS-based communication scheme must be capable of combining the transmitted energy, which was scattered over an arbitrary number of resolvable paths, and the mode of operation of the STS scheme can be adaptively controlled according to the receiver's detection performance.

When the number of resolvable paths is low and hence the resultant BER is higher than the required BER, then a low throughput STS-assisted transmitter mode is activated, which exhibits a high transmit diversity gain, as it will be demonstrated below with the aid of an example. By contrast, when the number of resolvable paths is high and hence the resultant BER is lower than the required BER, then

a higher throughput STS-assisted transmitter mode is activated, which has a lower transmit diversity gain.[2]

Specifically, the principle of implementing channel-dispersion-controlled adaptive rate transmission using adaptive STS may be readily interpreted by referring to the following example. Let the transmitter employ a total of four transmission antennas. If the number of resolvable paths experienced by the receiver is low, the transmitter is instructed by the receiver to employ an STS scheme based on four transmit antennas, using the STS scheme described as [21]

$$\mathbf{S} = [c_1\, c_2\, c_3\, c_4] \begin{pmatrix} b_1 & b_2 & b_3 & b_4 \\ b_2 & -b_1 & b_4 & -b_3 \\ b_3 & -b_4 & -b_1 & b_2 \\ b_4 & b_3 & -b_2 & -b_1 \end{pmatrix}, \qquad (36)$$

where c_1, c_2, c_3, c_4 are four STS-related orthogonal codes having a period of $4T_b$. The above STS scheme transmits $U = 4$ parallel data bits during the interval of $4T_b$, and hence the effective transmission rate becomes $R_b = 4 \times 1/4T_b = 1/T_b$, as seen in Figure 2. By contrast, when the number of resolvable paths increases, the transmitter is instructed by the receiver to employ four separate STS schemes, each based on two transmit antennas, as seen in Figure 4, which can be formulated as

$$\mathbf{S} = \begin{pmatrix} [c_1\, c_2] \begin{pmatrix} b_1 & b_2 \\ b_2 & -b_1 \end{pmatrix} & [c_3\, c_4] \begin{pmatrix} b_3 & b_4 \\ b_4 & -b_3 \end{pmatrix} \\ [c_1\, c_2] \begin{pmatrix} b_5 & b_6 \\ b_6 & -b_5 \end{pmatrix} & [c_3\, c_4] \begin{pmatrix} b_7 & b_8 \\ b_8 & -b_7 \end{pmatrix} \end{pmatrix}, \qquad (37)$$

which, again, constitutes the four independent two-antenna-based STS schemes $\mathbf{B}_2(t)$ of (3), where c_1, c_2, c_3, c_4 are the $U = 4$ STS-related orthogonal codes having a period of $2T_b$. Based on the above four two-antenna-assisted STS schemes, $U = 4$ parallel data bits are transmitted during the first $2T_b$-duration interval using the STS scheme $\mathbf{B}_2(t)$ of (3). Specifically, antennas 1 and 2 are activated with the aid of c_1, c_2, while activating antennas 3 and 4 using c_3, c_4, as portrayed in Figure 4. During the following $2T_b$-duration slot another

---

[2]The transmitter does not necessarily have to have the explicit knowledge of the number of resolvable paths, there is a range of other criteria, which may be used for controlling the activation of the different antenna configurations. Firstly, since most existing systems employ explicit training for estimating the channel's impulse response (CIR), the significant-energy CIR taps explicitly quantify the number of resolvable multipath components. Another practical metric that may be used for activating the required antenna configuration is the bit error ratio (BER) estimated, for example, by the channel decoder's soft metrics. When the estimated BER is higher than the target BER, the transmitter is instructed to increase its spreading gain and hence reduce its throughput, as well as vice versa. The activation regime has to be conservative for the sake of maintaining the target BER even if the BER was underestimated. Finally, the Doppler frequency does not dramatically affect the system's performance, since the *amount of dispersion*, that is, the CIR duration, changes only, when traversing from an indoor-type nondispersive environment to an outdoor scenario and then to a rural scenario, which may require 10 minutes for the dispersion to change substantially. However, the system's increased throughput is achieved at the cost of an increased complexity.

four data bits are transmitted using the same scheme as outlined above. Consequently, the above four two-antenna-based STS schemes transmit a total of eight data bits during two consecutive $2T_b$-duration time slots having a total duration of $4T_b$, and the effective transmission rate is now doubled to $2R_b$. Furthermore, if the number of resolvable paths is sufficiently high, which results in requiring no transmit diversity at all, then the four transmission antennas can transmit their information independently, as demonstrated in Figure 3 and the corresponding transmission mode can be described as

$$\mathbf{S} = \begin{pmatrix} c_1 b_1 & c_2 b_2 & c_3 b_3 & c_4 b_4 \\ c_1 b_5 & c_2 b_6 & c_3 b_7 & c_4 b_8 \\ c_1 b_9 & c_2 b_{10} & c_3 b_{11} & c_4 b_{12} \\ c_1 b_{13} & c_2 b_{14} & c_3 b_{15} & c_4 b_{16} \end{pmatrix}, \quad (38)$$

which implies that each of the 16 bits is transmitted independently using an antenna within a duration T_b, where c_1, c_2, c_3, c_4 are four orthogonal codes having a period of T_b, each mapped to one antenna. Explicitly, this scheme is capable of transmitting a total of 16 data bits during an interval of $4T_b$, and hence we achieve a transmission rate of $4R_b$, as exemplified in Figure 3.

The PDF of the delay spread in a wireless communication channel can be approximated by a negative exponential distribution given by [31]

$$f(\tau) = \frac{1}{T_m} \exp\left(-\frac{\tau - \tau_0}{T_m}\right), \quad \tau \geq \tau_0, \quad (39)$$

where the minimum delay τ_0 is the time required for the signal to propagate directly following the line of sight from the transmitter to the receiver, and T_m represents the mean square of the distribution, which is also the average value of the delay spread. Some typical examples of T_m in different environments are [25] $T_m < 0.1$ microseconds for an indoor environment, $T_m < 0.2$ microseconds for an open rural area, $T_m \approx 0.5$ microseconds for a suburban area, and $T_m \approx 3$ microseconds for a typical urban area. In (39), we let $\tau_r = (\tau - \tau_0)/T_c$. Then the PDF of τ_r can be expressed as

$$f(\tau_r) = \frac{1}{T_m/T_c} \exp\left(-\frac{\tau_r}{T_m/T_c}\right), \quad \tau_r \geq 0, \quad (40)$$

where T_m/T_c represents the average delay spread to chip-duration ratio, and $\lfloor T_m/T_c \rfloor + 1$—where $\lfloor x \rfloor$ represents the largest integer not exceeding x—is the average number of resolvable paths, which has been widely used in the performance analysis of DS-CDMA systems transmitting over multipath fading channels.

Let the number of resolvable paths associated with the reference signal be L_r. For DS-CDMA signals having a chip duration of T_c, the number of near-instantaneous resolvable paths $L_r = \lfloor (\tau - \tau_0)/T_c \rfloor + 1$ can be modelled as a discrete random variable, which varies slowly depending on the communication environment encountered. For a given BER, let the maximum throughput conditioned on the number of resolvable paths L_r be $B(L_r)$. Ideally, assuming that the receiver

is capable of combining an arbitrary number of resolvable paths and that the transmitter has the perfect knowledge of the number of resolvable paths with the aid of a feedback channel, and that the feedback delay is negligible, the unconditional throughput, B, using adaptive STS can be written as

$$B = \sum_{L_r=1}^{\infty} P(L_r) \cdot B(L_r), \quad (41)$$

where $P(L_r)$ is the probability that there are L_r resolvable paths at the receiver. With the aid of (40), this probability can be approximated as

$$\begin{aligned} P(L_r) &= \int_{\max\{0, L_r-1-0.5\}}^{L_r-1+0.5} f(\tau_r) d\tau_r \\ &= \int_{\max\{0, L_r-1-0.5\}}^{L_r-1+0.5} \frac{1}{T_m/T_c} \exp\left(-\frac{\tau_r}{T_m/T_c}\right) d\tau_r \\ &= \exp\left(-\frac{\max\{0, L_r-1-0.5\}}{T_m/T_c}\right) - \exp\left(-\frac{L_r-1+0.5}{T_m/T_c}\right), \end{aligned} \quad (42)$$

where $[L_r-1-0.5, L_r-1+0.5]$ is the normalised delay spread range having L_r resolvable paths. In (41), $B(L_r)$ represents the maximum possible throughput conditioned on having L_r number of resolvable paths. For example, for the proposed adaptive STS scheme using four-antenna-based STS, two-antenna-based STS, as well as conventional single-antenna-based transmission, as characterised in (36), (37), and (38), $B(L_r)$ may achieve values of R_b, $2R_b$, or $4R_b$, respectively, depending on the specific number of resolvable paths encountered.

Figures 10 and 11 show the throughput versus SNR/bit performance of the STS-assisted W-CDMA system using a maximum of four antennas. The maximum dispersion of the propagation environment was $T_m = 0.1, 0.2, 0.5$, and 3 microseconds. The corresponding number of resolvable multipath components at the 3.84 Mchip/s chip rate of the third-generation systems [3] became $(T_m/T_c) + 1 = 1, 2, 3$, and 16, respectively. Depending on the number of resolvable paths at the receiver and on the corresponding achievable BER performance, the transmitter may activate one of the transmission schemes described by (36), (37), and (38). In our related investigations, the target BER was set to 0.01. Specifically, if a sufficiently high number of resolvable paths is encountered by the receiver, which results in a BER of less than 0.01 for the scheme described by (38), then the transmitter supports a bitrate of $4R_b$. If the number of resolvable paths is in a range, where the BER using the scheme described by (38) is higher than 0.01, but that of the STS scheme described by (37) is lower than 0.01, then the transmitter transmits at a rate of $2R_b$. Finally, if the number of resolvable paths is in a range, where the BER using the STS scheme described by (37) is higher than 0.01, but that described by (36) is lower than 0.01, then the transmitter transmits at a rate of R_b. Otherwise, if the number of resolvable paths is too low, which results in BER > 0.01 for the STS scheme described by (36), then the transmitter simply disables transmissions.
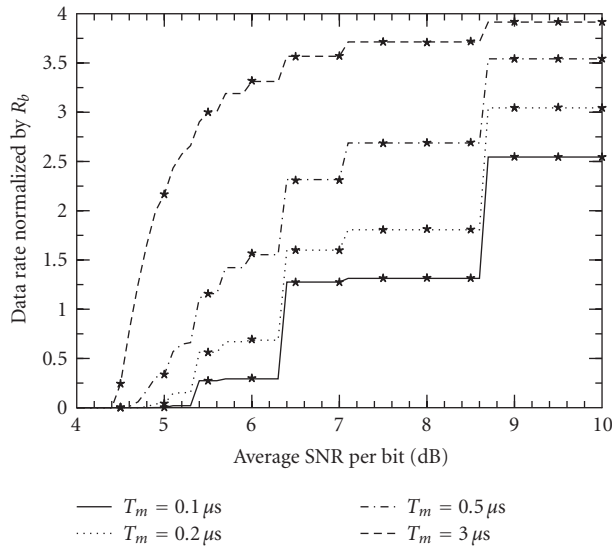
FIGURE 10: Normalized throughput versus the SNR per bit, E_b/N_0, performance of the adaptive space-time-spreading-assisted W-CDMA system using four-antenna-based STS of (36), the two-antenna-aided STS of (37), and the conventional single-antenna scheme for transmission over four typical wireless channels experiencing Rayleigh fading ($m = 1$). The target BER of the reference user is 0.01 and there are no interference users, that is, $K = 1$ ($G = 128, \eta = 0, R_{\text{chip}} = 3.686$ Mcps/s).
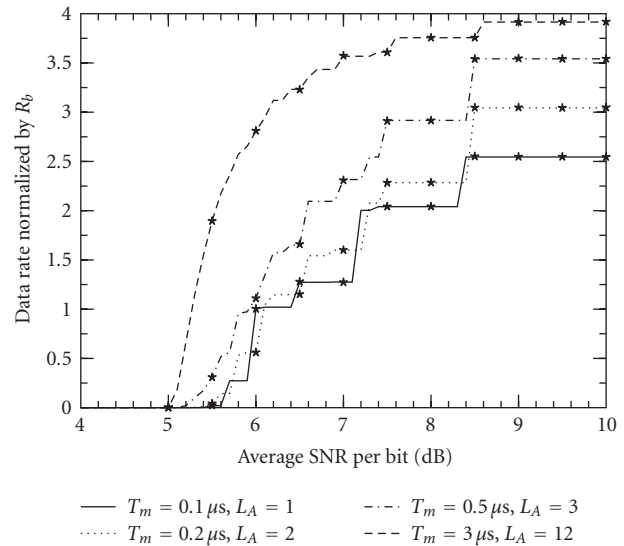

FIGURE 11: Normalized throughput versus the SNR per bit, E_b/N_0, performance of the adaptive space-time-spreading-assisted W-CDMA system using the four-antenna-based STS of (36), the two-antenna-aided STS of (37), and the conventional single-antenna scheme for transmission over four typical wireless channels obeying the Nakagami-m distribution ($m_1 = 2$, $m_c = 1$). The target BER of the reference user is 0.01, while the interfering users communicate using the four-antenna-based STS of (36) and each interfering signal has an average of L_A number of resolvable paths ($G = 128, K = 10, \eta = 0, R_{\text{chip}} = 3.686$ Mcps/s).

In the context of Figure 10 we assumed that the number of users was $K = 1$, and that the fading associated with each resolvable path obeyed the Rayleigh distribution ($m = 1$). By contrast, in Figure 11 we assumed that the number of users was $K = 10$, and that the fading associated with the first resolvable path obeyed the Nakagami-m distribution in conjunction with $m = 2$, while the fading of the other resolvable paths obeyed the Rayleigh distribution ($m_c = 1$).

From the results of Figures 10 and 11 we observe that with the aid of the adaptive STS scheme, the system's effective throughput is significantly increased, if the average delay spread of the channel is sufficiently high or, in other words, if the number of resolvable paths varies over a sufficiently wide range. We will highlight the significance of this observation in more detail. Using $T_m = 0.5$ microseconds and 3 microseconds as examples and by observing Figure 10 we find that the SNR/bit required for transmitting at the data rate of R_b is about 5.2 dB for $T_m = 0.5$ microseconds and 4.6 dB for $T_m = 3$ microseconds. Similarly, the SNR/bit required for supporting the data rate of $3R_b$ is about 6.4 dB for $T_m = 0.5$ microseconds and 5 dB for $T_m = 3$ microseconds. Hence, the adaptive STS-assisted W-CDMA system increased the achievable transmission rate by a factor of three, while requiring only a modest transmitted power increase of about 1.2 dB for $T_m = 0.5$ microseconds and 0.4 dB for $T_m = 3$ microseconds. Similar results can also be observed in Figure 11, where an extra 0.4 dB or 1.2 dB transmitted power is required for achieving a data rate of $3R_b$ instead of R_b. However, if

the number of resolvable paths varies over a relatively low range, the required increase of the transmitted power becomes higher. For example, for the case of $T_m = 0.1$ microseconds in Figures 10 and 11 an extra 2.2 dB (Figure 10) or 1.2 dB (Figure 11) transmitted power must be invested, in order to achieve a data rate of $2R_b$ instead of R_b. In this scenario, due to the associated extra complexity of the adaptive STS-assisted scheme required by the channel dispersion estimation and feedback, and due to the control channel requirement of the dispersion feedback, the adaptive STS-aided scheme might not constitute a more attractive alternative. The system's increased effective throughput ultimately leads to a potentially better speech [6] or video [7] service quality for the users of the system.

6. CONCLUSIONS

In this contribution, we have investigated the performance of STS-assisted W-CDMA systems, when multipath Nakagami-m fading, multiuser interference, and background noise-induced impairments are considered. Our analysis and numerical results demonstrated that the achievable diversity order is the product of the frequency selective diversity order and the transmit diversity order. Furthermore, both the transmit diversity and the frequency selective diversity have a similar influence on the BER performance of the W-CDMA systems considered. Since W-CDMA signals typically experience high-dynamic frequency-selective fading in both urban

and suburban areas, the proposed adaptive transmit diversity scheme will result into an increased throughput and ultimately in a potentially better speech [6] or video [7] service quality for the users of the system. Based on the above scenarios, we proposed an adaptive STS transmission scheme, which adapts its STS configuration using (36), (37), and (38) according to the frequency selectivity information fed back from the receivers. The numerical results show that by efficiently exploiting the channel's frequency selectivity, the proposed adaptive STS scheme is capable of significantly improving the throughput of W-CDMA systems. For W-CDMA systems transmitting at a data rate of $3R_b$ instead of R_b, only an extra of 0.4 dB and 1.2 dB transmitted power is required in the urban and suburban areas considered, respectively, which results in a substantially increased speech [6] or video [7] service quality. Alternatively, a potentially higher number of users may be supported within the same bandwidth, as a benefit of cross-layer optimisation.

A number of related open research problems may be identified, such as the design of more sophisticated STS-aided multicarrier CDMA transceivers. The design of new STS codes is also a promising research area. A particularly promising research topic is designing large area synchronous (LAS) STS schemes, which exhibit a so-called interference-free window (IFW). Provided that the interfering signals arrive within this IFW, no multiuser interference is inflicted. Finally, quantifying the achievable network-layer benefits [3] of STS-aided CDMA systems is an important open problem.

ACKNOWLEDGMENTS

REFERENCES

[1] L. Hanzo, C. H. Wong, and M. S. Yee, *Adaptive Wireless Transceivers: Turbo-Coded, Turbo-Equalized and Space-Time Coded TDMA, CDMA, and OFDM Systems*, John Wiley, New York, NY, USA, 2002.

[2] L. Hanzo, T. H. Liew, and B. L. Yeap, *Turbo Coding, Turbo Equalisation and Space-Time Coding for Transmission over Fading Channels*, John Wiley, New York, NY, USA, 2002.

[3] J. S. Blogh and L. Hanzo, *Third-Generation Systems and Intelligent Wireless Networking: Smart Antennas and Adaptive Modulation*, John Wiley, New York, NY, USA, 2002.

[4] L. Hanzo, M. Münster, B. J. Choi, and T. Keller, *OFDM and MC-CDMA for Broadband Multi-user Communications, WLANs and Broadcasting*, Wiley-IEEE Press, New York, NY, USA, 2003.

[5] L. Hanzo, L.-L. Yang, E.-L. Kuan, and K. Yen, *Single and Multi-Carrier DS-CDMA: Multi-User Detection, Space-Time Spreading, Synchronisation, Standards and Networking*, Wiley-IEEE Press, New York, NY, USA, 2003.

[6] L. Hanzo, F. C. A. Somerville, and J. P. Woodard, *Voice Compression and Communications: Principles and Applications for Fixed and Wireless Channels*, Wiley-IEEE Press, New York, NY, USA, 2001, http://www-mobile.ecs.soton.ac.uk.

[7] L. Hanzo, P. Cherriman, and J. Streit, *Wireless Video Communications: Second to Third Generation and Beyond*, IEEE Press, New York, NY, USA, 2001.

[8] ITU-T Rec. H.26L/ISO/IEC 11496-10, "Advanced video coding," September 2002.

[9] E. A. Brewer, R. H. Katz, Y. Chawathe, et al., "A network architecture for heterogeneous mobile computing," *IEEE Pers. Commun.*, vol. 5, no. 5, pp. 8–24, 1998.

[10] L. Tong, Q. Zhao, and G. Mergen, "Multipacket reception in random access wireless networks: from signal processing to optimal medium access control," *IEEE Commun. Mag.*, vol. 39, no. 11, pp. 108–112, 2001.

[11] A. J. Goldsmith and S. B. Wicker, "Design challenges for energy-constrained ad hoc wireless networks," *IEEE Wireless Communications Magazine*, vol. 9, no. 4, pp. 8–27, 2002.

[12] C. Comaniciu and H.V. Poor, "Jointly optimal power and admission control for delay sensitive traffic in CDMA networks with LMMSE receivers," *IEEE Trans. Signal Processing*, vol. 51, no. 8, pp. 2031–2042, 2003.

[13] S. Shakkottai, T. S. Rappaport, and P. C. Karlsson, "Cross-layer design for wireless networks," *IEEE Commun. Mag.*, vol. 41, no. 10, pp. 74–80, 2003.

[14] A. Maharshi, T. Tong, and A. Swami, "Cross-layer designs of multichannel reservation MAC under Rayleigh fading," *IEEE Trans. Signal Processing*, vol. 51, no. 8, pp. 2054–2067, 2003.

[15] V. Tarokh, N. Seshadri, and A. R. Calderbank, "Space-time codes for high data rate wireless communication: performance criterion and code construction," *IEEE Trans. Inform. Theory*, vol. 44, no. 2, pp. 744–765, 1998.

[16] V. Tarokh, H. Jafarkhani, and A. R. Calderbank, "Space-time block coding for wireless communications: performance results," *IEEE J. Select. Areas Commun.*, vol. 17, no. 3, pp. 451–460, 1999.

[17] A. F. Naguib, V. Tarokh, N. Seshadri, and A. R. Calderbank, "A space-time coding modem for high-data-rate wireless communications," *IEEE J. Select. Areas Commun.*, vol. 16, no. 8, pp. 1459–1478, 1998.

[18] S. M. Alamouti, "A simple transmit diversity technique for wireless communications," *IEEE J. Select. Areas Commun.*, vol. 16, no. 8, pp. 1451–1458, 1998.

[19] Proposed TDOC: 662/98 to ETSI SMG2 UMTS Standards, *Space-time block coded transmit antenna diversity for WCDMA*, December 1998.

[20] Telcomm. Industry Association (TIA), *TIA/EIA Interim Standard: Physical Layer Standard for cdma2000 Standards for Spread Spectrum Systems*, 2000.

[21] B. Hochwald, T. L. Marzetta, and C. B. Papadias, "A transmitter diversity scheme for wideband CDMA systems based on space-time spreading," *IEEE J. Select. Areas Commun.*, vol. 19, no. 1, pp. 48–60, 2001.

[22] T. Eng and L. B. Milstein, "Coherent DS-CDMA performance in Nakagami multipath fading," *IEEE Trans. Commun.*, vol. 43, no. 234, pp. 1134–1143, 1995.

[23] M. B. Pursley, "Performance evaluation for phase-coded spread-spectrum multiple-access communication-Part I: System analysis," *IEEE Trans. Commun.*, vol. 25, no. 8, pp. 795–799, 1977.

[24] J. G. Proakis, *Digital Communications*, McGraw-Hill, New York, NY, USA, 3rd edition, 1995.

[25] W. C. Y. Lee, *Mobile Communications Engineering*, McGraw-Hill, New York, NY, USA, 2nd edition, 1998.

[26] N. Nakagami, "The *m*-distribution, a general formula for intensity distribution of rapid fading," in *Statistical Methods in Radio Wave Propagation*, W. G. Hoffman, Ed., Pergamon, Oxford, England, 1960.

[27] V. Aalo, O. Ugweje, and R. Sudhakar, "Performance analysis of a DS/CDMA system with noncoherent M-ary orthogonal modulation in Nakagami fading," *IEEE Trans. Veh. Technol.*, vol. 47, no. 1, pp. 20–29, 1998.

[28] M.-S. Alouini and A. J. Goldsmith, "A unified approach for calculating error rates of linearly modulated signals over generalized fading channels," *IEEE Trans. Commun.*, vol. 47, no. 9, pp. 1324–1334, 1999.

[29] M. K. Simon and M.-S. Alouini, "A unified approach to the probability of error for noncoherent and differentially coherent modulations over generalized fading channels," *IEEE Trans. Commun.*, vol. 46, no. 12, pp. 1625–1638, 1998.

[30] M. K. Simon and M. Alouini, "A unified approach to the performance analysis of digital communication over generalized fading channels," *Proc. IEEE*, vol. 86, no. 9, pp. 1860–1877, 1998.

[31] L. E. Miller and J. S. Lee, *CDMA Systems Engineering Handbook*, Artech House, Boston, Mass, USA, 1998.

Lie-Liang Yang received his M.Eng and Ph.D. degrees in communications and electronics from Northern Jiaotong University, Beijing, China, in 1991 and 1997, respectively, and his B.Eng. degree in communications engineering from Shanghai Tiedao University, Shanghai, China, in 1988. Since December 1997, he has been with the Communications Research Group at the Department of Electronics and Computer Science, University of Southampton, UK, where he held various research posts as a Visiting Postdoctoral Research Fellow, Research Fellow, and Senior Research Fellow. He currently holds an academic post as a Lecturer. From June 1997 to December 1997 he was a Visiting Scientist of the IREE, The Academy of Sciences of the Czech Republic. He has been involved in a number of projects funded by the National Science Foundation of China, the Grant Agency of the Czech Republic, the Engineering and Physical Sciences Research Council (EPSRC) of UK, and the European Union. His research covers a wide range of areas in communications, which include data network and security, intelligent wireless networking, error control coding, modulation and demodulation, spread-spectrum communications and multiuser detection, pseudonoise (PN) code synchronisation, smart antennas, adaptive wireless systems, as well as wideband, broadband, and ultra-wideband code-division multiple access (CDMA) for advanced wireless mobile communication systems. He has published over 90 papers in various journals and conference proceedings. He is a Senior Member of the IEEE.

Lajos Hanzo, a Fellow of the Royal Academy of Engineering (FREng), received his Master's degree in electronics in 1976 and his Doctorate in 1983. In 2004, he was awarded the Doctor of Sciences (D.S.) degree from the University of Southampton, UK. During his 28-year career in telecommunications he has held various research and academic posts in Hungary, Germany, and the UK. Since 1986 he has been with the Department of Electronics and Computer Science, University of Southampton, UK, where he holds the Chair in telecommunications. He has coauthored 11 John Wiley/IEEE Press books totalling about 8000 pages on mobile radio communications, published in excess of 500 research papers, organised and chaired conference sessions, presented overview lectures, and has been awarded a number of distinctions. Currently he is managing an academic research team, working on a range of research projects in the field of wireless multimedia communications sponsored by industry, the Engineering and Physical Sciences Research Council (EPSRC), UK, the European IST Programme, and the Mobile Virtual Centre of Excellence (VCE), UK. He is an enthusiastic supporter of industrial and academic liaison and he offers a range of industrial courses. Dr. Hanzo is also an IEEE Distinguished Lecturer of both the Communications Society and the Vehicular Technology Society as well as a Fellow of both the IEEE and IEE. For further information on research in progress and associated publications, please refer to http://www-mobile.ecs.soton.ac.uk.